Systems & Control Transactions

Original Research Article
Peer Reviewed Conference Proceeding
ESCAPE 36 - European Symposium on Computer Aided Process Engineering
Sheffield, UK. 21-24 June 2026

PSE PRESS

Capturing mixing effects on aggregation kinetics of monoclonal antibodies during viral inactivation

T. Marella[a], F. Cenci[b], P. Thompson[c], M. Muhieddine[b], F. Bezzo[a]*

[a] CAPE-Lab – Computer-Aided Process Engineering Laboratory. Department of Industrial Engineering. University of Padova, Padova, Italy.
[b] GSK Ware Research and Development, Ware, UK.
[c] GSK R&D, Biopharmaceutical Drug Substance Development (BDSD), King of Prussia, USA.
* Corresponding Author: fabrizio.bezzo@unipd.it

ABSTRACT

Mathematical models play a central role in biopharmaceutical manufacturing, especially within the Quality by Design framework. For these models to be effectively used in optimization tasks, they must be both reliable and capable of delivering results in an affordable computational time. This work proposes a strategy to model aggregate formation during viral inactivation in the context of monoclonal antibody downstream processing. These units often display mixing-sensitive behavior because aggregation kinetics is controlled by local pH, whose spatial heterogeneities arise from titrant addition at a defined feed point. To address this challenge, compartment models (CMs) are employed. This modeling approach captures spatial inhomogeneities within the unit by leveraging flow-exchange information derived from a single steady-state Computational Fluid Dynamics (CFD) simulation involving only the solution of mass, momentum and turbulence equations. Results obtained by comparing compartment models with both perfectly mixed models and full CFD simulations including aggregation kinetics demonstrate that CMs can reproduce the CFD results with good approximation, while reducing computational time by orders of magnitude.

Keywords: Compartment Models, Computational Fluid Dynamics, Monoclonal Antibodies, Downstream Bioprocessing

INTRODUCTION

Mathematical modeling has become a cornerstone in the modernization of pharmaceutical manufacturing, enabling process optimization, quality-by-design strategies, and the development of digital twins [1]. To effectively serve this role, models must ensure robustness and reproducibility under real manufacturing conditions, especially because this level of reliability is increasingly required by regulatory frameworks.

Beyond supporting unit-operation design, mathematical models are equally essential at the system level, where they allow the integrated optimization of process configurations, resource allocation, and operational strategies.

Achieving this goal calls for an accurate description of the relevant phenomena across multiple scales, from process-level behavior down to local fluid dynamics [2]. This aspect is particularly critical in unit operations where fluid flow and mixing have a decisive impact on process outcomes.

In the context of biopharmaceutical manufacturing for monoclonal antibodies (mAb) production, one of the most critical operations where mixing plays a central role is the viral inactivation step. This step takes place in the downstream section of the process, during which purification and product quality refinement are carried out. This operation is designed to ensure product safety by lowering the solution pH through the addition of an acidic titrant and holding this condition for a minimum amount of time, thereby inactivating acid-labile viruses. However, low pH conditions simultaneously trigger aggregation kinetics for certain monoclonal antibodies [3]. Aggregation is a key risk, as it may impact product quality and reduce yield, and its kinetics depend strongly on the local pH distribution within the vessel. Therefore, spatial heterogeneities in mixing directly translate into variations in aggregation rates, linking hydrodynamics with critical

quality attributes, especially for proteins that are prone to low-pH aggregation.

A model of the unit in which the viral inactivation step is performed must therefore be able to capture the influence of imperfect mixing on both pH distribution and aggregation kinetics in order to provide reliable and accurate predictions. Additionally, the application of a unit model inside process-level optimization tasks requires the capability of this model to provide predictions within a significantly reduced computational time. This combination of physical fidelity and computational efficiency is essential to enable model-based decision-making in biopharmaceutical development and manufacturing.

Due to their simplicity and fast computational times, models that assume perfectly mixed conditions inside the vessel are commonly used in process-level optimization tasks. However, these models fail to represent the effect of fluid dynamics on the aggregation kinetics, leading to an underestimation of aggregation risks and potentially misleading performance predictions. On the other hand, when a detailed hydrodynamic description is required, computational fluid dynamics (CFD) models that solve both the flow behavior and the transport of species are generally employed. While this kind of approach can be highly accurate, it requires substantially higher computational time and resources, which limits its applicability for system-level optimization and for extensive exploration of complex physical phenomena [4].

To overcome the challenge of developing hydrodynamics-oriented yet time-efficient models, a multi-scale approach should be adopted for the modeling of the vessel. One promising way to implement such a multi-scale strategy is through compartment models (CMs). In this modeling approach, the vessel is discretized into a network of interconnected compartments, each assumed to be ideally mixed [5]. The exchange of mass between compartments is not modeled directly by solving the full fluid-flow equations, but is instead derived from a single CFD simulation that solves only the flow and turbulence equations [6]. This makes it possible to capture the large-scale hydrodynamics at a reduced computational cost, while retaining spatial heterogeneities and flow non-idealities within the equipment. Compartment models therefore provide a powerful intermediate between overly simplified ideal-mixing assumptions and the full resolution of CFD simulations [7][8][9]. This makes them particularly useful for describing the pH distribution inside the unit and, in turn, its effect on aggregation kinetics at a significantly reduced computational cost.

This work aims to examine the applicability of compartment modeling to the viral inactivation step in mAb production processes, with the goal of developing a model that incorporates local pH gradients to improve predictive accuracy compared to perfectly mixed models, while providing results in a substantially shorter time than a full CFD simulation. Such a model can be readily used for process-level optimization or for evaluating alternative operating conditions that do not affect the underlying fluid dynamics.

MODELING WORKFLOW

The modeling workflow adopted in this study is described in this section.

The development of the compartment model follows a sequential procedure. First, a CFD simulation resolving only the fluid flow (momentum, continuity, and turbulence equations) is performed. The process geometry is then discretized into compartments, after which the mass-flow exchanges between compartments are computed from the CFD results. Finally, the corresponding material balances are solved. The following sections detail each step of this workflow.

Fluid flow only CFD simulation

A steady-state CFD simulation resolving the fluid flow (momentum, continuity, and turbulence equations) serves as the starting point for the development of the compartment model.

Two different vessel geometries representative of equipment used during industrial viral inactivation at different scales are here considered. Comparing these two configurations allows to investigate how vessel geometry and characteristic scales influence mixing patterns, pH distribution, and consequently aggregation behavior.

The first geometry, referred to as the *R&D scale* vessel, consists of a cylindrical unbaffled tank with a conical bottom and a maximum working volume of 200 L, operated here with 90L of liquid. The nominal impeller speed is set to 230 RPM. The second geometry, referred to as the *Clinical scale* vessel, features a square cross-sectional area and a maximum working volume of 1000 L, and it is operated with 550L of liquid. The nominal impeller speed is set to 180 RPM.

An unstructured polyhedral mesh was selected for the simulations of both geometries. The meshes were generated using Ansys® Fluent, release 25.1 watertight geometry meshing workflow. The resulting meshes comprise 377348 computational cells for the *R&D scale* vessel and 1261684 cells for the *Clinical scale* one. CFD simulations were run using Ansys® Fluent, release 25.1.

The fluid inside the vessel comes the prior purification step. It contains the product, process impurities, and buffer components. The density is 1007 kg/m^3, while the viscosity is 10^{-3} Pa·s.

To model turbulence, the SST k-ω model is selected, retaining the default parameters. To model the impeller rotation, the Multiple Reference Frame approach is used; the rotating reference frame is shown in Figure 1 for the *R&D scale* vessel and in Figure 2 for the *Clinical*

scale one.

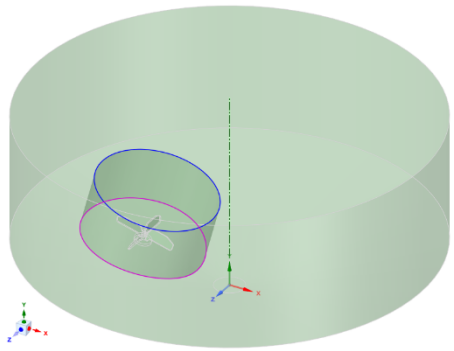

Figure 1. 3D geometry of the *R&D scale* vessel.

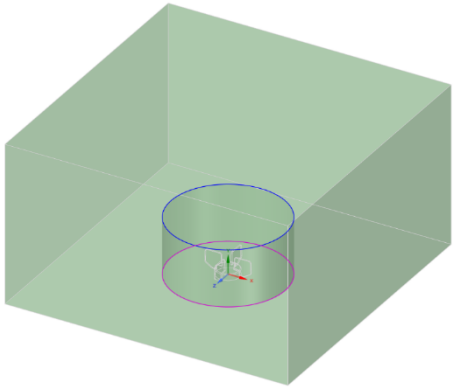

Figure 2. 3D geometry of the *Clinical scale* vessel.

The simulations are performed under steady-state conditions and the resulting fluid-flow behavior was validated against experimental operating data from the vessel, using blend time as the metric for comparison.

Key information required to build the compartment model (e.g. cell centroid coordinates, volume, velocity components, data concerning neighbouring cells) are exported in text files using User Defined Functions.

Compartment model

Starting from the results of the steady-state CFD simulation describing the detailed fluid flow behavior, the compartment model is built through a sequence of steps: first, the geometry is divided into compartments; next, the fluxes between compartments are computed; and finally, the material balances within each compartment are solved. All implementations were carried out in a Python 3.13 environment.

Compartmentalization

The compartmentalization procedure is the preliminary step in constructing the compartment model. Its purpose is to divide the system geometry into compartments, each representing a volume in which the perfectly mixed assumption is applied. Adjacent compartments are then allowed to exchange mass with one another.

In this study, a basic compartmentalization procedure is employed. More complex approaches, e.g. accounting for the flow patterns inside the tank, can be found in the literature [10][11][12].

The selected compartmentalization procedure consists of defining the number of compartments to be generated along the different coordinate axes. In this way, the system is compartmentalized so that all compartments have approximately the same volume. Due to the distinct geometries of the two vessels, a cylindrical coordinate system (r, θ, y) was used for the *R&D scale* tank whereas a cartesian coordinate system (x, y, z) was adopted for the *Clinical scale* tank. An example of compartment division with 4 compartments along each coordinate is visualized in Figure 3 using cylindrical coordinates for the *R&D scale* vessel, in Figure 4 using cartesian coordinates for the *Clinical scale* one.

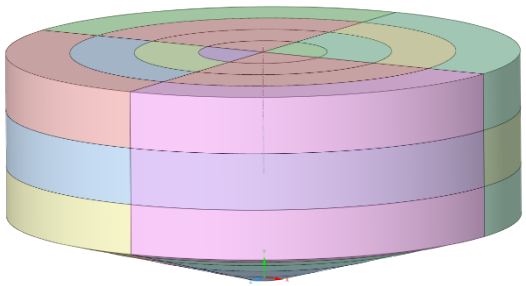

Figure 3. Example of compartmentalization with four compartments along the different coordinates for the *R&D scale* vessel using cylindrical coordinates.

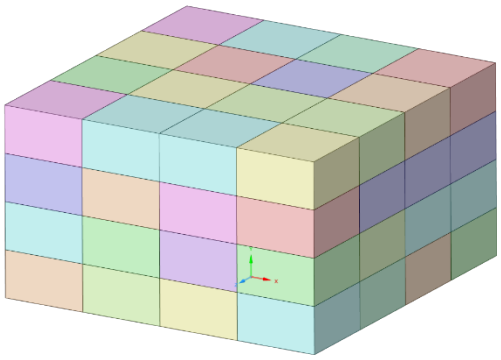

Figure 4. Example of compartmentalization with four compartments along the different coordinates for the *Clinical scale* tank using cartesian coordinates.

After this subdivision, the CFD mesh cells are grouped based on whether their centroids fall within the coordinate bounds of each compartment [13]. Consequently, at the end of this step, a mapping is obtained that associates each CFD mesh cell with its corresponding compartment.

Fluxes computation

To compute the material exchanges between compartments, the face flux data exported from the CFD

simulation are used. For each mesh face *k*, the CFD solver provides a flux value f_k.

Faces that connect cells belonging to two different compartments are identified by examining the compartments associated with their neighboring CFD cells. Let compartment *i* contain the set of CFD mesh cells $\mathcal{C}_i$, and compartment j the set $\mathcal{C}_j$. A face *k* contributes to the exchange between compartments *i* and *j* if it connects a cell $c_a \in \mathcal{C}_i$ and a cell $c_b \in \mathcal{C}_j$. Based on this identification, the set of faces contributing to the flux from compartment *i* to compartment *j* can be defined as:

$$\mathcal{F}_{i\to j} = \{k \mid k \text{ connects a cell in } \mathcal{C}_i \text{ to a cell in } \mathcal{C}_j\} \quad (1)$$

A schematic illustrating how cells and faces are assigned to each set is shown in Figure 5.

The total flux from compartment *i* to compartment *j* is then computed as the sum of the corresponding face fluxes:

$$F_{i\to j} = \sum_{k\in\mathcal{F}_{i\to j}} f_k \quad (2)$$

Consequently, the overall outgoing and incoming fluxes for compartment *i* are defined as:

$$F_i^{out} = \sum_{j=1}^{N} F_{i\to j} \quad (3)$$

$$F_i^{in} = \sum_{j=1}^{N} F_{j\to i} \quad (4)$$

where *N* is the total number of compartments.

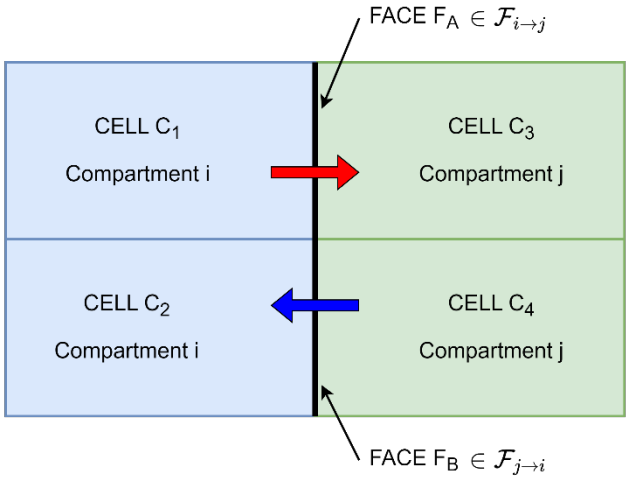

Figure 5. Schematics of assignments of cells and faces. $C_1, C_2 \in \mathcal{C}_i, C_3, C_4 \in \mathcal{C}_j$. Face F_A divides cells $C_1 \in \mathcal{C}_i$ and $C_3 \in \mathcal{C}_j$, and is assigned to set $\mathcal{F}_{i\to j}$ since mass flux is from C_1 to C_3; face F_B divides cells $C_2 \in \mathcal{C}_i$ and $C_4 \in \mathcal{C}_j$, and is assigned to set $\mathcal{F}_{j\to i}$ since mass flux is from C_4 to C_2.

Material balances

The compartment model then solves a system of ordinary differential equations, composed of one equation per species in each compartment. The mass balances are expressed as follows:

$$\frac{dM_{i,c}}{dt} = \sum_{k=1}^{N}(F_{k\to c} * w_{k,i}) - w_{c,i} * F_{c,outgoing} + R \quad (5)$$

where $M_{i,c}$ is the mass of species *i* in compartment *c*, *N* is the total number of compartments, $w_{c,i}$ is the mass fraction of species *i* in compartment *c*, *R* represents reaction or source terms for species *i* in compartment *c*.

The resulting system of material balances is solved using the *solve_ivp* function from the *scipy* library, with the BDF method selected as the numerical solver.

The solution returns the mass profiles of each species within all compartments as a function of time. To enable comparison across different models, the total mass of each species in the tank is then computed at every timestep by summing its mass over all compartments.

All simulation results will be compared to that of a perfectly mixed tank.

CASE STUDY

Some monoclonal antibodies are prone to aggregation under low-pH conditions. A simplified kinetic expression describing this behavior was derived from the work of Arosio et al. (2011) [3]. The simplified aggregation mechanism can be represented as:

$$M + M \xrightarrow{k_{aggr}} A \quad (6)$$

The kinetic constant k_{aggr} is assumed to depend on pH according to the following relationship:

$$k_{aggr} = \left(k^0_{aggr}\right) \cdot \exp\left(-\beta(pH - 3.334)\right) \quad (7)$$

where k^0_{aggr} and β are model parameters estimated from experimental data. Their numerical values are reported in Table 1.

Table 1: Aggregation kinetics model parameters.

Parameter	Value
k^0_{aggr}	4.518 [m³/(kg h)]
β	8.468 [-]

The reaction rate can therefore be expressed on a mass basis as:

$$R = k_{aggr} \cdot [M]^2 \quad (8)$$

where *[M]* is the mass concentration of the mAb.

All kinetic expressions were formulated on a mass basis to simplify their implementation in the CFD simulations, since no information on the molecular weight of the mAb was available.

To incorporate the aggregation kinetics into both the CFD simulations and the compartment models, three species must be considered: the monoclonal antibody, referred to as the monomer; the product formed through aggregation, referred to as the aggregate; and the

oxonium ion, which is included to represent the pH distribution inside the tank through its definition:

$$pH = -\log_{10}[H_3O^+] \quad (9)$$

where $[H_3O^+]$ is the molar concentration of oxonium ion expressed in mol/L. Since the total fluid density is assumed to remain constant, an additional species, referred to as the solvent, is considered implicitly. Its mass is not obtained by solving a dedicated balance equation; instead, it is computed at each time step as the difference between the total fluid mass and the sum of the masses of all explicitly modeled species.

The viral inactivation process operates in fed-batch mode, as a titrant is continuously added to the vessel to reduce the pH to the desired target value. In principle, this would result in a time-varying liquid volume inside the tank. However, to simplify the set up of the simulations, the process was modeled under the assumption of constant volume.

In the CFD simulations, the reaction rate is implemented as a source term for monomer or aggregate in all fluid zones using Equation (5). The continuity, momentum, and turbulence equations were not solved during this stage, and the flow variables were fixed to the values obtained from the initial steady-state simulation.

All simulations were carried out in transient mode. The simulations were initialized using typical values reported in experimental studies of aggregation kinetics for pH, monomer concentration, and aggregate concentration. These initial conditions were assumed to be homogeneous throughout the vessel volume. The process was simulated until the pH reached the final target value, corresponding to a decrease of 1.55 relative to the initial condition.

RESULTS

This section presents the main results obtained in assessing the performance of the compartment models, comparing them against both the perfectly mixed models and the CFD simulations. The CFD results are taken as the most representative approximation of real process behavior, as no experimental data were available for direct validation.

For the compartment model, different numbers of compartments were investigated in order to evaluate how the degree of geometric discretization influences the model predictions. The number of compartments selected along each coordinate is reported in Table 2. At the finest discretization level, the total number of compartments differs between the *R&D scale* and *Clinical scale* vessels due to the conical bottom of the *R&D scale* tank, which results in some compartments containing no CFD mesh cells and therefore being excluded from the model.

Table 2: Different degrees of compartmentalization considered.

Number of compartments			Tot. comp.
x/r	y	z/θ	
2	2	2	8
4	4	4	64
8	4	8	256
12	8	12	1152 (Clin.) 1068 (R&D)

Two scenarios were considered in the performance assessment. In the first scenario, a slow titrant addition was modeled: the amount of titrant required to reach the target pH was fed over a 30 minutes interval. The simulation was then run for a total of 35 minutes to allow both the addition to be completed and the pH to homogenize throughout the tank. In the second scenario, the titrant was added over a 0.5 seconds interval, representing an almost instantaneous addition. In this case, the simulations were performed over a 35 seconds time window to ensure that mixing and pH homogenization could be observed across the entire vessel. The second scenario, characterized by a fast titrant addition, was included because it is expected to generate stronger local inhomogeneities within the tank. This, in turn, is anticipated to amplify the differences in the predictions obtained from the different modeling approaches.

Scenario 1: Slow titrant addition

The time profiles of the total monomer mass inside the vessel, normalized with respect to the initial value, as predicted by the different models for the first scenario, are shown in Figure 6 for the *R&D scale* vessel and in Figure 7 for the *Clinical scale* one.

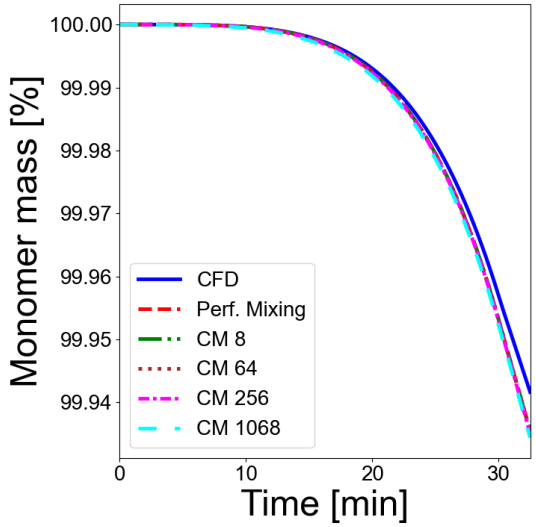

Figure 6. Scenario 1: total monomer mass profiles for the R&D scale vessel.

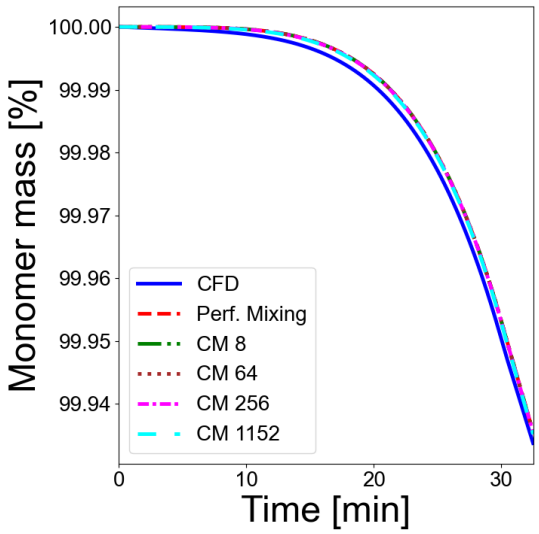

Figure 7. Scenario 1: total monomer mass profiles for the *Clinical scale* vessel.

The profiles obtained with the perfectly mixed model and the compartment models are nearly identical and closely match the CFD results, with discrepancies below 0.01%. This means that for scenario 1 both vessels behave as perfectly mixed systems. Consequently, in this scenario, both CFD and compartment models do not provide a strategic advantage with respect to the perfectly mixed model in predicting the unit behavior.

Scenario 2: Fast titrant addition

The time profiles of the total monomer mass inside the vessel, normalized with respect to the initial value, as predicted by the different models for the second scenario, are shown in Figure 8 for the *R&D scale* vessel and in Figure 9 for the *Clinical scale* one.

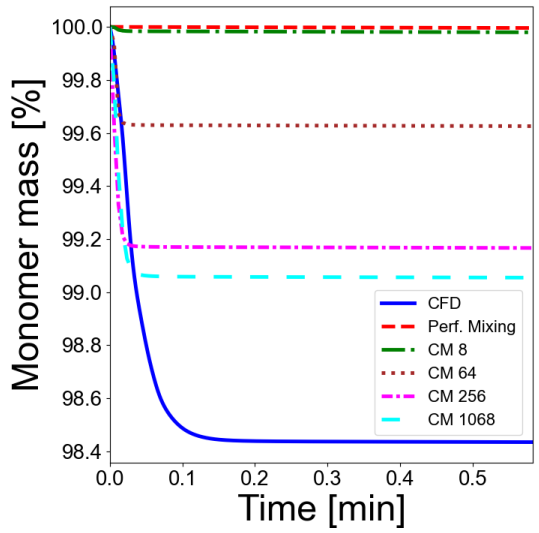

Figure 8. Scenario 2: total monomer mass profiles for the *R&D scale* vessel.

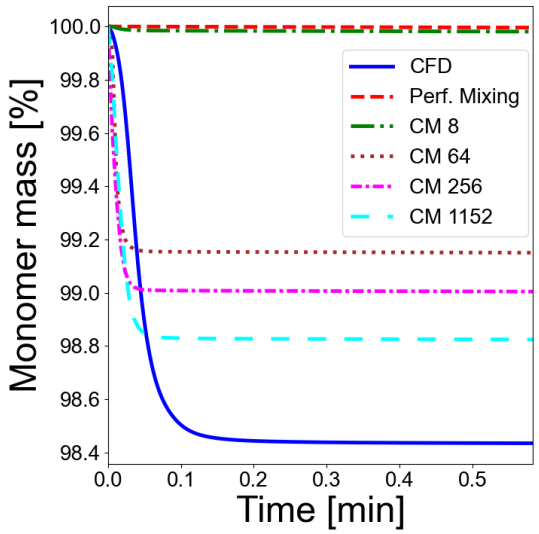

Figure 9. Scenario 2: total monomer mass profiles for the *Clinical scale* vessel.

As expected, this second scenario in which the titrant is added almost instantaneously inside the tank leads to the formation of pronounced localized pH inhomogeneities within the tank. These local variations are inherently captured by the CFD simulations but are not represented by the perfectly mixed model, which assumes instantaneous homogenization throughout the vessel. As a consequence, in this second scenario the CFD simulation predicts a pronounced initial aggregation that is not captured by the perfectly mixed approach. The compartment models, on the other hand, are able to reproduce this early aggregation behavior with increasing accuracy, as their predictions progressively approach the CFD results when a finer level of compartment discretization is employed.

Table 3 reports the computational times for both the R&D scale and the Clinical scale vessels.

Table 3: Computational times for the model solution under the fast titrant addition scenario.

Model	Computational time	
	R&D scale	Clinical scale
CFD	16.75 [h]	75 [h]
Perf. Mixed	0.05 [s]	0.05 [s]
CM 8	0.05 [s]	0.05 [s]
CM 64	0.13 [s]	0.16 [s]
CM 256	1.17 [s]	1.51 [s]
CM 1068 or 1152	39.40 [s]	56.30 [s]

A substantial reduction in computational cost can be observed: while the CFD simulations required days, the compartment models provided the predictions in less than a minute at the highest level of discretization, and in less than two seconds for the coarser discretizations. The reported computational times do not include the

duration of the preliminary steps required for model preparation, as these must be performed only once before the model can be repeatedly solved. The preliminary steady-state CFD simulations, required for both the CFD runs and the compartment models with kinetics included, took approximately 4 hours for the R&D-scale vessel and 8 hours for the clinical-scale vessel. The compartmentalization step took approximately 5 seconds, independent of the discretization level and the vessel scale.

CONCLUSIONS

This study explored the integration of fluid-flow information obtained from CFD simulations into modeling frameworks that require significantly lower computational effort. The proposed procedure was applied to a viral inactivation process within the context of downstream biopharmaceutical manufacturing.

The results demonstrated that compartment models are able to provide predictions that are closer to the CFD results than those obtained with perfectly mixed models, while requiring substantially less computational time. This makes these models suitable for system-level optimization studies and, more generally, for scenarios in which multiple simulations are needed.

These models also offer the capability to rapidly evaluate different process operating conditions, provided that such variations do not affect the underlying fluid-flow behavior.

Opportunities for further improvement lie primarily in the compartmentalization procedure, where more advanced techniques could enhance both model performance and reliability.

ACKNOWLEDGEMENTS

T.M. and F.B. acknowledge GSK R&D for financial support.

DECLARATION OF COMPETING INTEREST

The authors declare the following financial interests/personal relationships which may be considered as potential competing interests: F. Cenci, M. Muhieddine and P. Thompson are employees of GSK and may hold share options and/or shares in GSK. The authors declare no other competing conflicts of interest.

AUTHOR IDENTIFIERS

Author ORCIDs:
Tiziana Marella: 0009-0008-3119-7818
Francesca Cenci: 0000-0002-3360-0470
Fabrizio Bezzo: 0000-0003-1561-0584

REFERENCES

1. Destro F, Barolo M. A review on the modernization of pharmaceutical development and manufacturing – trends, perspectives, and the role of mathematical modeling. International Journal of Pharmaceutics 620:121715 (2022). https://doi.org/10.1016/j.ijpharm.2022.121715
2. Jaworski Z, Zakrzewska B. Towards multiscale modelling in product engineering. Computers & Chemical Engineering 35:434-445 (2011). https://doi.org/10.1016/j.compchemeng.2010.05.009
3. Arosio P, Barolo G, Müller-Späth T, Wu H, Morbidelli M. Aggregation stability of a monoclonal antibody during downstream processing. Pharm Res 28:1884-1894 (2011). https://doi.org/10.1007/s11095-011-0416-7
4. Le Nepvou De Carfort J, Pinto T, Krühne U. An automatic method for generation of cfd-based 3D compartment models: towards real-time mixing simulations. Bioengineering 11:169 (2024). https://doi.org/10.3390/bioengineering11020169
5. Jourdan N, Neveux T, Potier O, Kanniche M, Wicks J, Nopens I, Rehman U, Le Moullec Y. Compartmental modelling in chemical engineering: a critical review. Chemical Engineering Science 210:115196 (2019). https://doi.org/10.1016/j.ces.2019.115196
6. Bezzo F, Macchietto S, Pantelides CC. A general methodology for hybrid multizonal/cfd models. Computers & Chemical Engineering 28:501-511 (2004). https://doi.org/10.1016/j.compchemeng.2003.08.004
7. Delafosse A, Collignon ML, Calvo S, Delvigne F, Crine M, Thonart P, Toye D. Cfd-based compartment model for description of mixing in bioreactors. Chemical Engineering Science 106:76-85 (2014). https://doi.org/10.1016/j.ces.2013.11.033
8. Farzan P, Ierapetritou MG. A framework for the development of integrated and computationally feasible models of large-scale mammalian cell bioreactors. Processes 6:82 (2018). https://doi.org/10.3390/pr6070082
9. Maldonado de León H, Straathof A, Haringa C. Dynamic compartment models: towards a rapid modeling approach for fed-batch fermentations. Chemical Engineering Science 308:121396 (2025). https://doi.org/10.1016/j.ces.2025.121396
10. Tajsoleiman T, Spann R, Bach C, Gernaey KV, Huusom JK, Krühne U. A CFD based automatic method for compartment model development. Computers & Chemical Engineering 123:236-245 (2019).

https://doi.org/10.1016/j.compchemeng.2018.12.015
11. Laborda VPI, Puiman L, Groves T, Haringa C, Nielsen LK. Unsupervised learning bioreactor regimes. Computers & Chemical Engineering 194:108891 (2025). https://doi.org/10.1016/j.compchemeng.2024.108891
12. Le Nepvou De Carfort J, Puig I Laborda V, Nielsen LK, Gernaey KV, Krühne U. Flow-informed clustering of bioreactor volumes to build cfd-based compartment models. Chemical Engineering Science 320:122539 (2026). https://doi.org/10.1016/j.ces.2025.122539
13. Haringa C, Tang W, Noorman HJ. Stochastic parcel tracking in an euler–lagrange compartment model for fast simulation of fermentation processes. Biotech & Bioengineering 119:1849-1860 (2022). https://doi.org/10.1002/bit.28094

© 2026 by the authors. Licensed to PSEcommunity.org and PSE Press. This is an open access article under the creative commons CC-BY-SA licensing terms. Credit must be given to creator and adaptations must be shared under the same terms. See https://creativecommons.org/licenses/by-sa/4.0/